

EFFECT OF THE PEAK PHASE DELAY ON AN ACOUSTO – OPTIC INTERACTIONS

Alwan M.Alwan^{*}, Duha S. Ahmed^{**}, Uday N.Saleman and Israa S. Ahmed

School of Applied Sciences, University of Technology, Baghdad, Iraq.

^{*}*Alkrzsm@yahoo.com.*

^{**}*Melak_duniamzs@yahoo.com.*

Abstract

In this work, introducing the relation between peak phase delay (α) and laser intensity at different values of Klein–Cook (Q) of the fourth order of diffraction, a numerical model was obtained to describe the light–sound interaction in the LiNbO₃ crystal in absence of feedback. Mean while, the relations between laser intensity with the acoustic frequency, values of (Q) parameter and laser incidence angle.

Keyword: Acousto-optic, Acousto-optic interaction, peak phase delay

Introduction

The Acousto-optic (AO) effect is the diffraction of laser beam by sound waves, was first predicted independently by Brillouin in 1921[1,6]. This effect can be described qualitatively as follows: an ultrasonic wave propagating through a solid or liquid may locally cause compression and rarefaction to the medium. This compression and rarefaction is known as a photo elastic effect, which may induce changes in the refractive index of the medium.

Periodically alternating layers with different refractive indices are thus formed in the medium, since the ultrasonic sound wave is sinusoidal in nature. These layers move at the velocity of sound and are separated by half the acoustic wavelength. When light is incident at a certain angle, called Bragg angle, onto a medium and propagates through the above-mentioned periodic structure, this is known as Bragg diffraction [2].

The acousto-optic modulator consists of a small block of crystal or glass to which a piezoelectric transducer is bonded. When a voltage waveform is applied to the transducer, a traveling acoustic wave is generated within the acousto-optic medium. In this state, the AOM can be used to deflect, diffract, modulate, or otherwise manipulate a coherent light beam such as that supplied by a laser [2,7,8].

This paper presents a simple acousto-optic (AO) interaction without feedback. Mathematical and analytical models describing

the AO interaction were studied and differential equations were numerically solved using MATLAB.

Modeling the Acousto-optic Phenomena with Wave-Vector Diagrams:

The model of acousto-optic interactions considers the physics of collisions between light photons and sound phonons. As in classical collisions, momentum must be conserved when both photon and a phonon collide. The conservation of momentum can be expressed mathematically as [3]:

$$\hbar\mathbf{k}_{+1} = \hbar\mathbf{k}_0 + \hbar\mathbf{k} \dots\dots\dots (1)$$

Where, $\hbar = h/2\pi$ (h represents Planck's constant), and \mathbf{k}_{+1} , \mathbf{k}_0 , and \mathbf{k} represent the wave vectors of scattered light, incident light, and sound, respectively. Dividing by \hbar gives

$$\mathbf{k}_{+1} = \mathbf{k}_0 + \mathbf{k} \dots\dots\dots (2)$$

Likewise, applying the law of conservation of energy to a photon-phonon collision results in

$$\omega_{+1} = \omega_0 + \Omega \dots\dots\dots (3)$$

Where, ω_{+1} , ω_0 , and Ω are the angular frequencies of diffracted light, incident light, and sound, respectively. The diffracted light is up-shifted by the frequency of the sound, which accounts for the positive subscript of the diffracted wave vector. Downshifted diffraction is developed similarly. The conservation of momentum equation and energy equations for downshifted diffraction are

$$\mathbf{k}_{-1} = \mathbf{k}_O - \mathbf{K} \dots\dots\dots (4)$$

and

$$\omega_{-1} = \omega_O - \Omega \dots\dots\dots (5)$$

respectively.

These relationships are illustrated with ray diagrams in Figs. (1a) and (1b). Because $|k_0| \gg |K|$ in all practical cases, the wave vector triangles are nearly isosceles. Given this geometry, it is clear that for the interaction to produce a diffracted order, $k_{\pm 1}$, k_0 , and K must be related by a certain critical angle, labeled θ_B in the wave vector diagrams. This angle is called the Bragg angle and is seen to be :

$$\theta_B = \sin^{-1}\left(\frac{K}{2k_0}\right) = \sin^{-1}\left(\frac{\lambda}{2\Lambda}\right) \dots\dots\dots (6)$$

The wave vector diagram illustrates so-called Bragg diffraction, of which the defining feature is the creation of a two diffracted orders of light as shown in Fig. (2). In order to facilitate the classification of acousto-optic devices, the Klein-Cook parameter, Q , has been defined as:

$$Q = \frac{K^2 L}{k_0 \Lambda^2} = \frac{2\pi\lambda L}{\Lambda^2} \dots\dots\dots (7)$$

Where λ and Λ are both referenced inside of the acousto-optic medium and L is length of the crystal. A device is said to be operating in the Bragg regime for $Q > 1$.

The Plane Wave Interaction Model

A more complete mathematical model of acousto-optic interactions than either the diffraction grating or wave-vector diagram representations is the multiple plane wave interaction model. The theory represents the light and sound fields as plane wave decompositions and describes their interaction as a multiple scattering of plane waves. According to the theory, the complex amplitude of the n-th order diffracted plane wave propagating along $\theta_n = \theta_{inc} + 2n\theta_B$, \tilde{E}_n , is given by the following set of infinitely-linked, complex differential equations [4,5]:

$$\begin{aligned} \frac{d\tilde{E}_n}{d\zeta} = & -j\frac{\hat{\alpha}}{2} \exp\left\{\frac{-jQ\zeta}{2}\left[\frac{\theta_{inc}}{\theta_B} + (2n-1)\right]\right\} \tilde{E}_{n-1} \dots (8) \\ & - j\frac{\hat{\alpha}}{2} \exp\left\{\frac{jQ\zeta}{2}\left[\frac{\theta_{inc}}{\theta_B} + (2n+1)\right]\right\} \tilde{E}_{n+1} \end{aligned}$$

Where, α represents the peak phase delay through the medium and is given by $\alpha=Ck_0SL/2$ where C is the strain-optic coefficient of the medium and S is the amplitude of the sound wave propagating along the x-direction ζ is the normalized position inside the acousto-optic cell and is equal to z/L in the case of light propagating in the z-direction through a cell of length L . Finally, θ_{inc} is the angle of the incident plane wave.

A set of equations that only accounts for four diffracted orders can also be extracted from equation (1-8):

$$\begin{aligned} \frac{dE_{-1}}{d\zeta} = & -j\frac{\hat{\alpha}}{2} \exp\left[\frac{jQ\zeta}{2}\left(\frac{\theta_{inc}}{\theta_B} - 1\right)\right] E_0 \\ \frac{dE_0}{d\zeta} = & -j\frac{\hat{\alpha}}{2} \exp\left[\frac{jQ\zeta}{2}\left(\frac{\theta_{inc}}{\theta_B} - 1\right)\right] E_{-1} \\ & - j\frac{\hat{\alpha}}{2} \exp\left[\frac{jQ\zeta}{2}\left(\frac{\theta_{inc}}{\theta_B} + 1\right)\right] E_0 \\ \frac{dE_1}{d\zeta} = & -j\frac{\hat{\alpha}}{2} \exp\left[\frac{jQ\zeta}{2}\left(\frac{\theta_{inc}}{\theta_B} + 1\right)\right] E_0 \\ & - j\frac{\hat{\alpha}}{2} \exp\left[\frac{jQ\zeta}{2}\left(\frac{\theta_{inc}}{\theta_B} + 3\right)\right] E_1 \\ \frac{dE_2}{d\zeta} = & -j\frac{\hat{\alpha}}{2} \exp\left[\frac{jQ\zeta}{2}\left(\frac{\theta_{inc}}{\theta_B} + 3\right)\right] E_1 \end{aligned}$$

With initial condition
 $E_0(\zeta=0) = E_{inc}$, $E_1(0) = 0$, $E_{-1}(0) = 0$
 and $E_2(0) = 0$

Simulation Results

The solutions of the four-order system are difficult to be obtained analytically. The Runge-Kutta numerical method for solving boundary value problems was chosen for the task of solving the four-order diffraction problem because it is easy to implemented from scratch in MATLAB because of it is high accuracy.

The simulation result for four-order diffraction is shown in Fig. (3a). It shows that the predicted intensity of the zero diffraction across the first maximum intensities when the Cook-Klein parameter applied at a value about

one. The intensity of the first order diffraction is slightly little increases than those of others diffraction orders. This is because of some light being diffracted into the minus first and second orders as well. Subsequent intensity peaks of the first order are become lower as more and more light gets diffracted into higher orders.

This result can be easily verified by summing the intensities of non-zero orders as shown in Fig. (3b). The result, of course, should be exactly equal to the incident intensity (in our simulations $I_{inc} = 1$). The amount of variation from this value can be used to calculate the error introduced by the numerical method used to solve the equations system.

Fig. (4) shows the relationship between maximum peak phase delay and the Klein-Cook parameter for first order diffraction. This figure indicates that the maximum peak phase delay (α) decays exponentially as the Klein-Cook parameter (Q) increases.

The Klein-Cook parameter can be used in the four-order diffraction modeling to determine the operating device. Fig. (5) shows the simulation result of the Klein-Cook (Q), which shows the two-operation mode of the AOC. For, $Q < 1$, the first order diffraction intensity increases approximately linearly with Klein-Cook parameter.

For, $Q > 1$, however, the first order intensity approaches a maximum value and then remains nearly constant as the frequency increases.

As compared with the other diffraction orders, the intensity decreases to zero as shown in Fig. (6).

Another behavior of the AOM that can be molded using the four-order diffraction equations is to show the effect of the light incident angle of the AOM on the intensity of the first order diffraction. The variation of incident angle with the first order intensity can be modeled by MATLAB program to carry out Runge-Kutta analysis in order to determine this variation as shown in Fig. (7).

First, it is clear that from the Fig. (7), the first order intensity will be maximized when $\theta_{inc} = -\theta_B$, as expected. Second, the Bragg diffraction criterion can be determined. This condition can be met when $\theta_{inc} = -\theta_B$, which is approximately equal to the condition for Bragg diffraction given in terms of the Klein-Cook parameter. At different values of the Klein-Cook parameter, the maximum diffraction intensity increases with the Klein-Cook parameter increases as shown in Fig. (8).

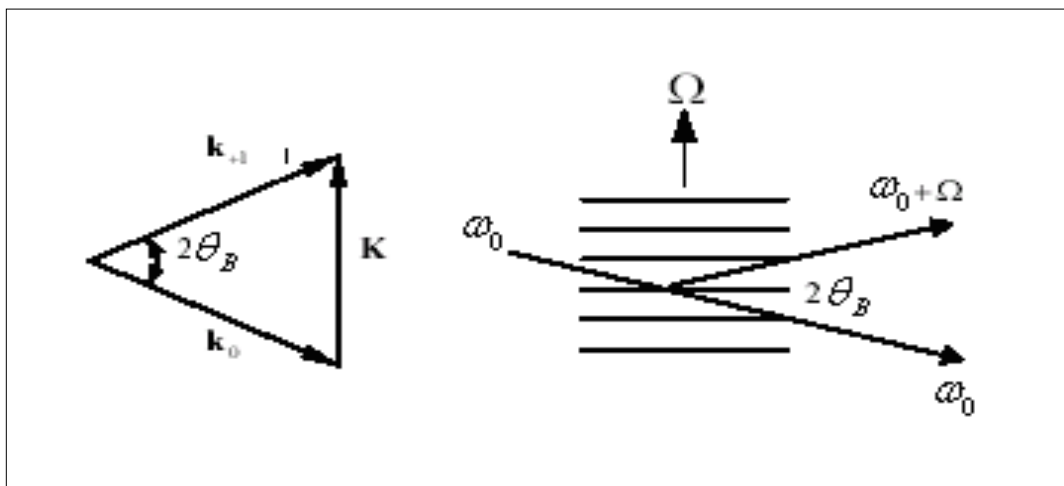


Fig. (1a) : Wave-vector diagram of up shifted ideal Bragg diffraction.

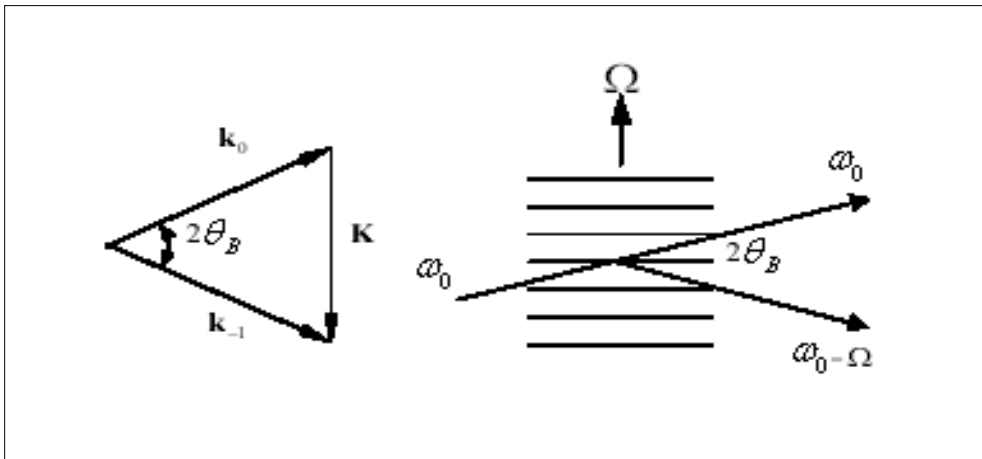


Fig. (1b) : Wave-vector diagram of downshifted ideal Bragg diffraction.

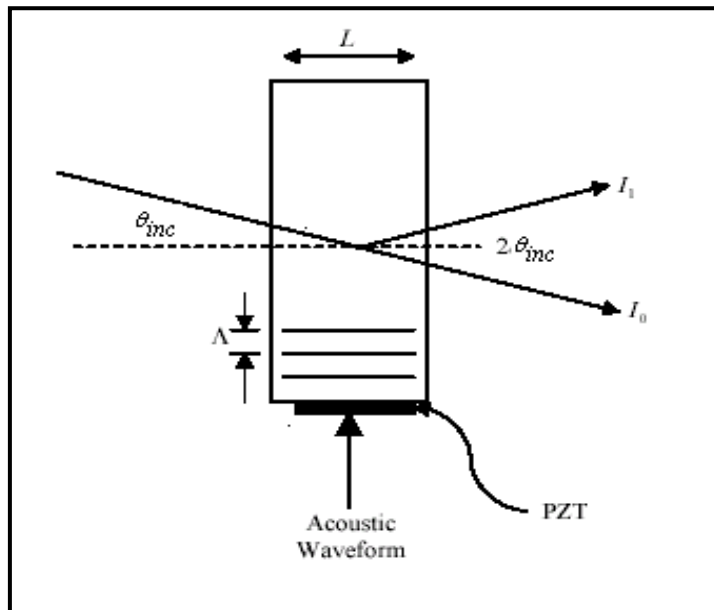
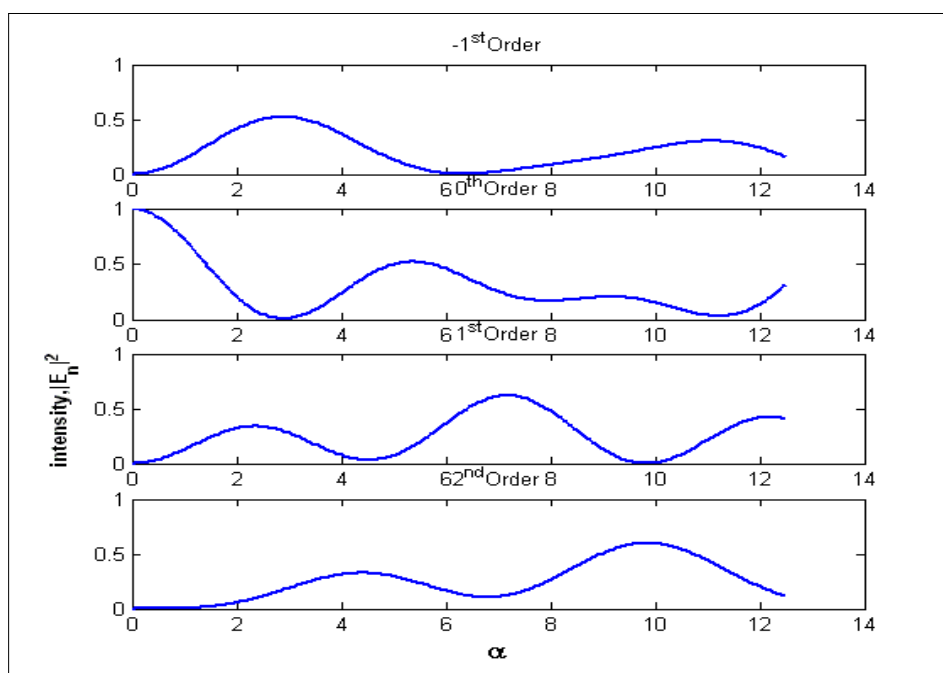
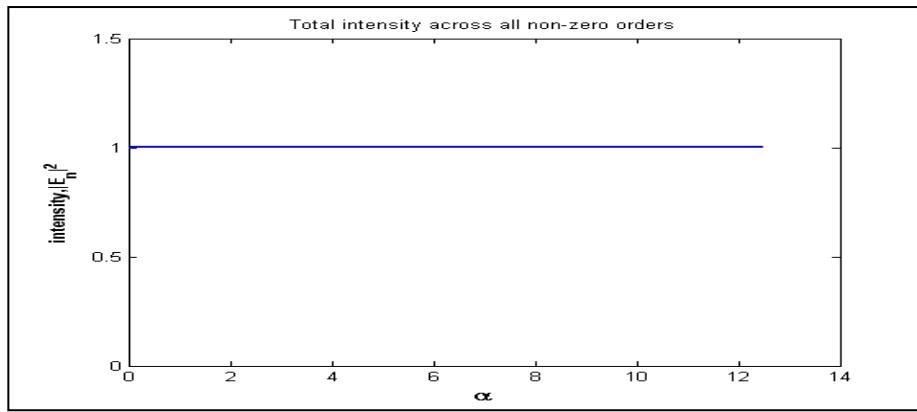


Fig. (2) : Bragg diffraction.



(a)



(b)

Fig. (3) : Solution for (a) Four-orders diffraction at $Q=1$ and (b) Total intensity across all non-zero.

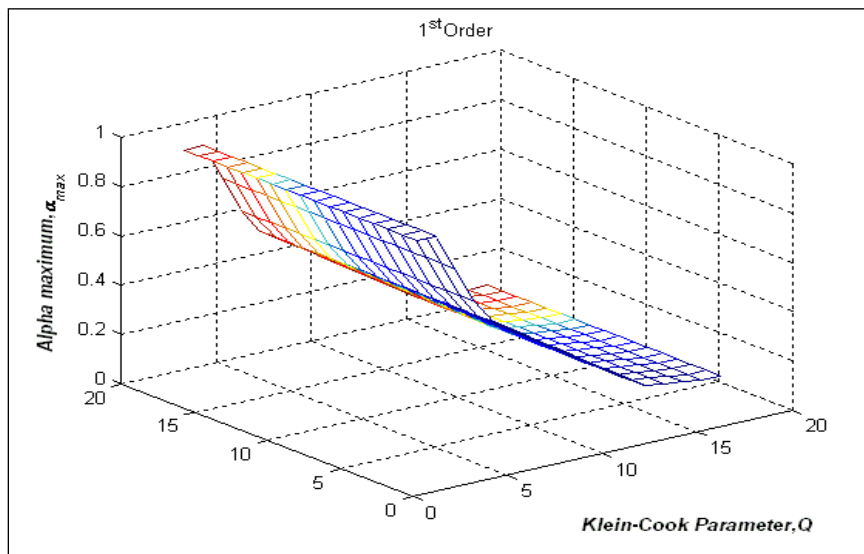


Fig. (4): Shows the relationship between maximum peak phase delay and the Klein-Cook parameter for first order diffraction.

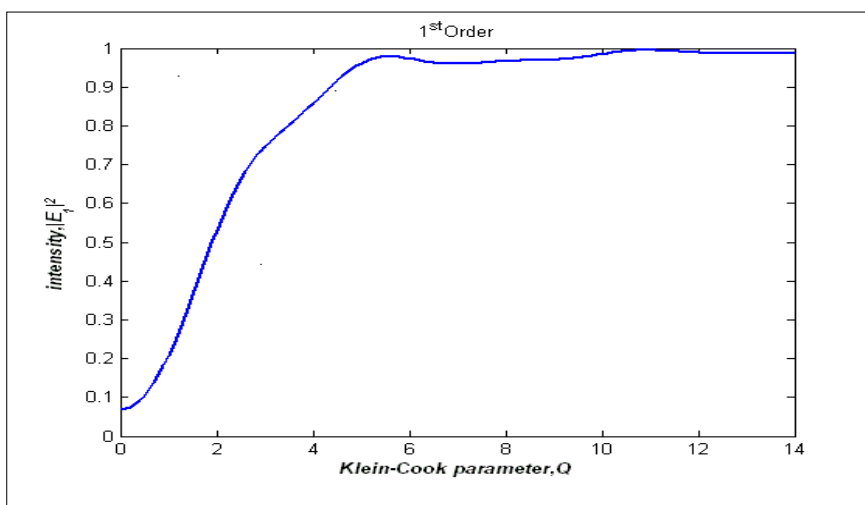


Fig. (5) : First order intensity versus the Klein-Cook parameter.

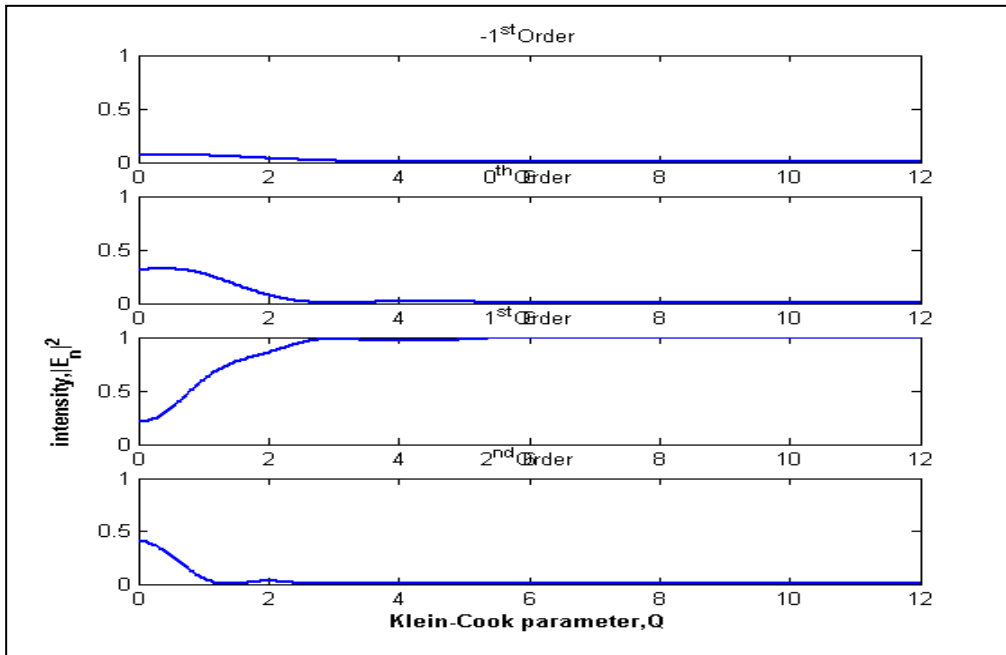


Fig. (6) : First order intensity versus the Klein-Cook parameter.

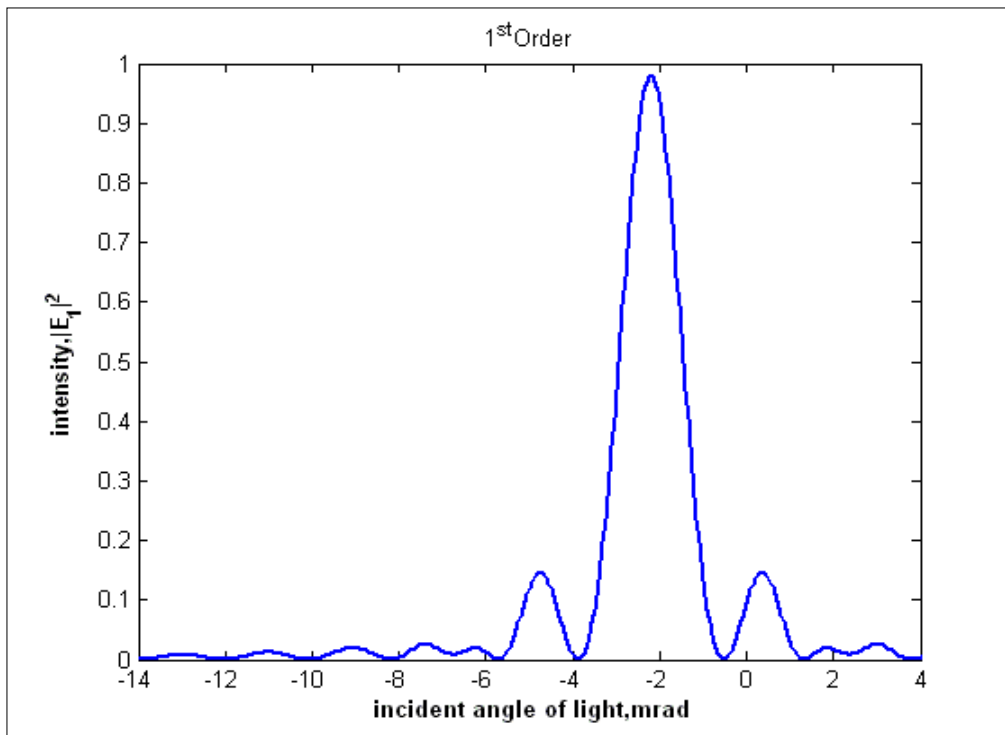
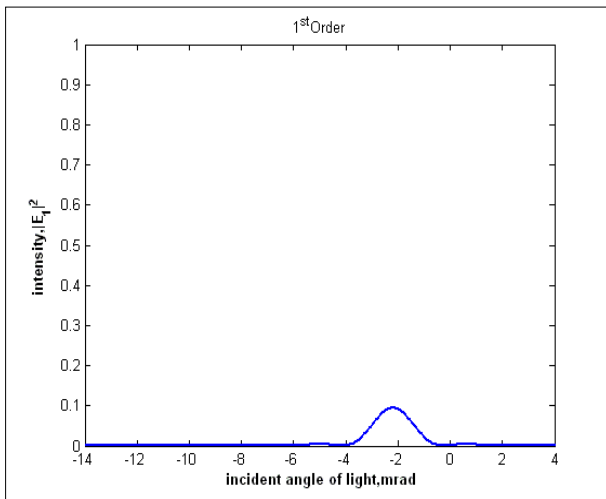
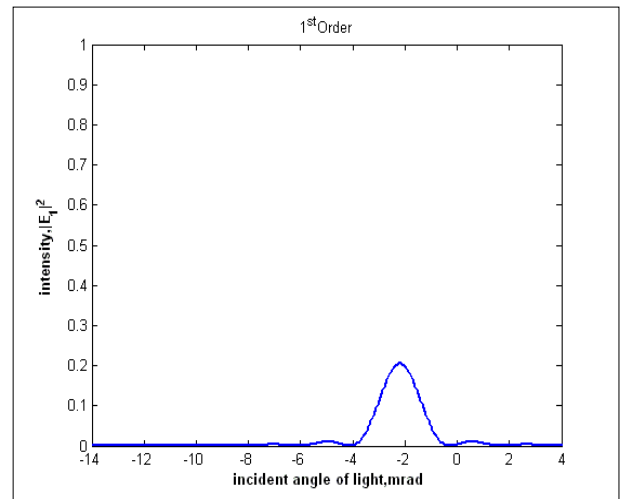


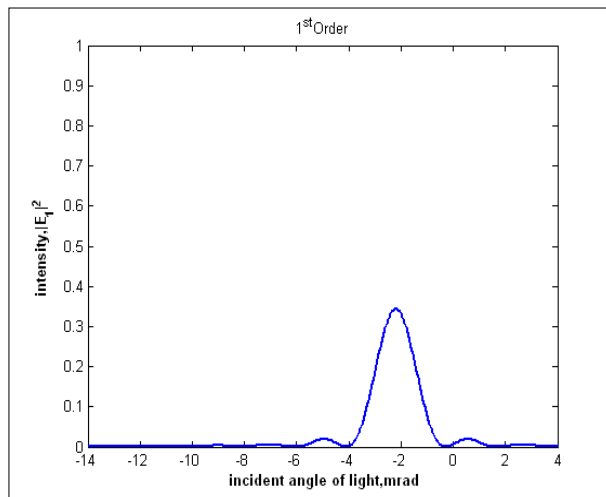
Fig. (7) : First order intensity versus incident angle at Q=14.



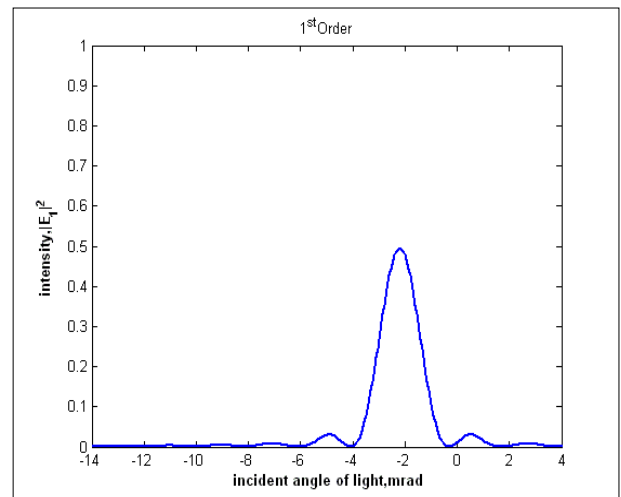
(a)



(b)

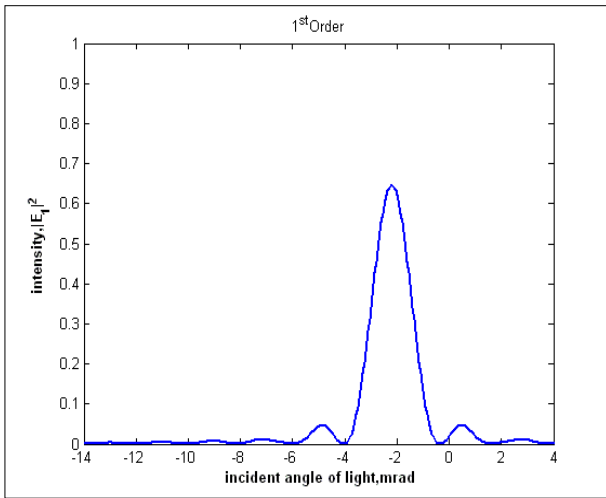


(c)

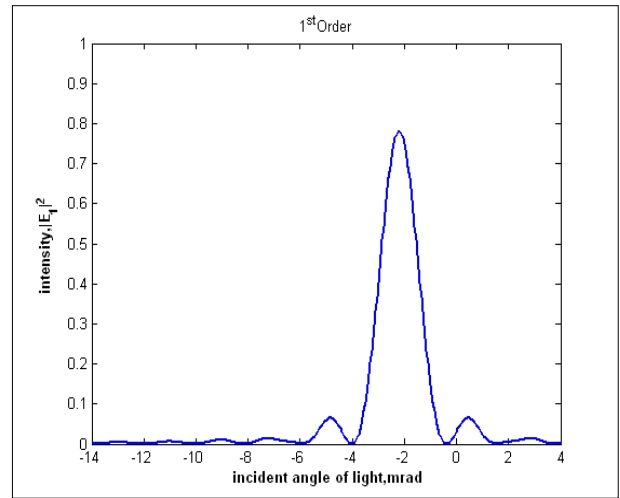


(d)

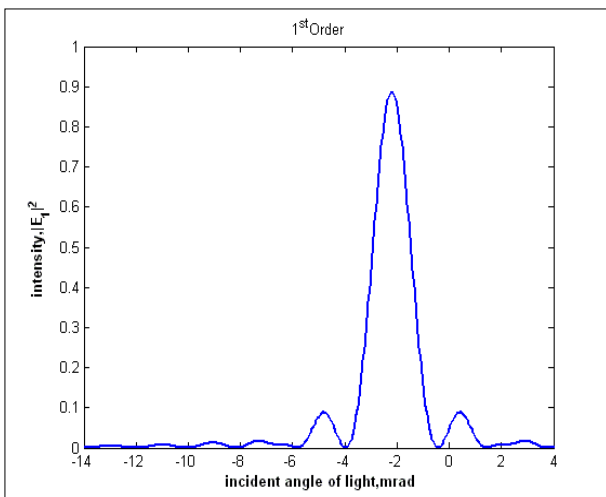
Fig. (8) : First order intensity versus incident angle with: (a) $Q=1$, (b) $Q=3$, (c) $Q=5$, (d) $Q=6$.



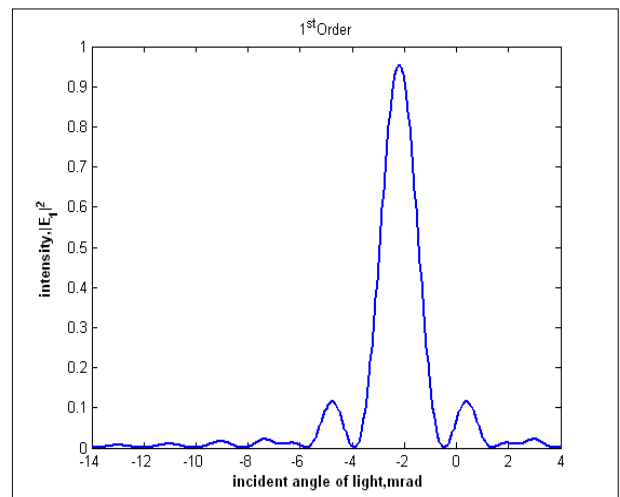
(a)



(b)



(c)



(d)

Fig. (9) : First order intensity versus incident angle with: (a) $Q=8$, (b) $Q=9$, (c) $Q=11$, (d) $Q=12$.

Conclusions

AO interaction was simulated and compared with different values of Klein-Cook parameter using MATLAB. For, $Q < 1$, the first order diffraction intensity increases approximately linearly with Klein-Cook parameter. As compared with the other diffraction orders, the intensity decreases to zero .

Reference

- [1] Korpel .A., "Acousto-optics, a Review of Fundamentals," Proc. IEEE vol. 69, 1981.
- [2] Arshia Cont, T.-C. Poon," Simulations of Bistable Acousto-Optic Devices Using MATLAB", Virginia Tech,2003.
- [3] Berg, N.J., and Lee. J.N.,Acousto-optic Signal Processing, Theory and Implementation, Marcel Dekker, 1983.
- [4] Banerjee, P. P., Poon, T.-C., 1990," Principles of Applied Optics", New York:Richard D. Irwin,.
- [5] Korpel, A.," Two-Dimensional Plane Wave Theory of Strong Acousto-optic Interaction in Isotropic Media", 1979, J. Opt. Soc.Am.,vol.69.
- [6] <http://www.aaoptoelectronic.com>.
- [7] Nakada M., Kawakami T.," Application of electronic Device for Aerosol Deposition Methods", NEC Technical journal, Vol. 2, No.1, 2007.
- [8] Strobl C., Wixforth A.,"Mikro-and Nan fluidic on piezoelectric substrate", University of Augsburg, 2002.

الخلاصة

أجري هذا البحث لتبيان العلاقة بين تغير الفاصلة الطورية وشدة حزمة الليزر لقيم عديدة من المعامل (Q) ضمن الرتبة الرابعة من الحيود. وقد تمكنا من الحصول على نموذج رياضي يصف تفاعل الضوء مع الصوت داخل بلورة لأخطية وفي حالة انعدام التغذية المردة. فيما جرى تحديد علاقة الشدة مع التردد الصوتي وقيم المعامل (Q) وزاوية سقوط شعاع الليزر على البلورة اللاخطية عند المرتبة الاولى من الحيود.